FACETING OF HIGH ANGLE GRAIN BOUNDARIES IN THE COINCIDENCE LATTICE†

Wilfried R. Wagner*, T. Y. Tan** and R. W. Balluffi**

November 16, 1973
Cornell University
Ithaca, New York 14850

Report #2133
Issued by
The Materials Science Center

† This work was supported by the U. S. Atomic Energy Commission under Contract AT(11-1)3158. Additional support was received from the National Science Foundation through the Materials Science Center at Cornell University.

* Now at Bell Telephone Laboratories, Murray Hill, New Jersey 07974

** Department of Materials Science and Engineering, Cornell University, Ithaca, New York 14850.

DISCLAIMER

ABSTRACT

Faceting of high angle grain boundaries in $\Sigma=3$ and $\Sigma=5$ coincidence lattices of the fcc structure was studied using thin-film bicrystal specimens of controlled geometry. A number of relatively high index boundaries in the coincidence lattices (containing relatively low planar densities of coincidence sites) was found to break up into low energy facets corresponding to low index planes of the coincidence lattices (containing high densities of coincidence lattice sites). These results are consistent with our general expectation that the grain boundary energy decreases as the planar density of coincidence sites increases, i.e., the two-dimensional periodicity of the boundary becomes shorter, and long-ranged distortions are reduced.

1. INTRODUCTION

In the coincidence lattice model for high angle grain boundaries (Brandon 1966, Bollmann 1970, Hirth and Balluffi 1973) a coincidence lattice is defined which consists of the infinite 3-dimensional array of points in space where a fraction, $1/\Sigma$, of the atoms of the two crystals which adjoin the grain boundary coincide, it it is imagined that both crystal lattices extend indefinitely in all directions. The 3-dimensional periodicity of the overall distribution of the atoms of the two interpenetrating crystals is therefore identical to that of the coincidence lattice. However, it has been pointed out that in the actual bicrystal relaxations may occur at the grain boundary which cause one crystal to translate rigidly (without rotation) with respect to the other crystal in a manner to eliminate the actual coincidence of atoms on the coincidence lattice points (Chalmers and Gleiter 1971, Bruggeman and Bishop 1973). If this happens it can be easily verified that the basic periodicity of the distribution of the atoms of the two crystals remains unchanged. A coincidence lattice, which is geometrically identical to that described above, can then be constructed in which equivalent unit cell positions (not necessarily occupied by atoms) in the first crystal lattice then coincide with a second and generally different set of equivalent unit cell positions in the second crystal lattice. The coincidence lattice, generalized in this way, therefore, depends only upon the relative orientations of the two adjoining crystals and is independent of their relative translational positioning.*

There is considerable evidence (Aust 1967, Balluffi, Komen and Schober 1972, Gleiter and Chalmers 1972) that the energy of a high angle grain boundary is relatively low whenever the orientation of the two grains is such that a coincidence lattice of rather small spacing is formed and when the boundary orientation is such that it passes through a high density plane of the coincidence lattice.† The atomic structure in the boundary is then 2-dimensionally periodic and possesses the same periodicity as the coincidence site lattice plane. Apparently, the relatively low energy in such cases is mainly the result of the short wave length periodicity of the boundary and the absence of long range distortions (Bruggeman and Bishop 1973). When the misorientation of the two adjoining crystals deviates somewhat from the high density coincidence lattice orientation it has been shown (Balluffi, Komen and Schober 1972) that secondary grain boundary dislocations (GBD's) are formed in order to produce a fit-misfit boundary structure in which a large fraction of the boundary area is restored to the short wave length periodic interface of low energy which is characteristic of the nearby exact high density coincidence lattice orientation.

---

* Alternatively, we may state that it is always possible to find a 3-dimensional point lattice (i.e., the generalized coincidence lattice) for which each lattice point is surrounded by an identical arrangement of atoms of the two interpenetrating real lattices. This result is independent of any relative translations of the two lattices.

† An extreme example is the well known case of the low energy coherent {111} twin in the fcc structure (see ABEF in Fig. 1)

On the basis of these considerations we would expect faceting to occur in many boundaries when the crystal orientation is near a high density coincidence lattice orientation but when the average grain boundary plane does not lie parallel to a high density plane of the coincidence lattice. In such cases the boundary should presumably be able to reduce its energy by breaking up into low energy facets which lie parallel to suitable high density planes of the coincidence lattice. Under these conditions the increase in grain boundary area is more than compensated for by the low energy per unit area of the facets.

A number of observations of grain boundary faceting have been reported (Weinberg 1969: Bishop, Hart and Bruggeman 1971: Weins and Weins 1972: also, see references in Gleiter and Chalmers 1972). In several of the above investigations the results can be understood on the basis of facets which are composed of short period coincidence structural units corresponding to near-coincidence conditions (Bruggeman, Bishop and Hartt 1972). The classic example of faceting in a coincidence lattice consists of boundaries between crystals in the twinned orientation in the fcc structure which often contain facets lying parallel to {111} which is the highest density plane in the coincidence lattice in this system (see Fig. 49 in Amelinckx and Dekeyser 1959). However, no systematic studies of faceting in coincidence lattices have yet been performed.

In the present work we have carried out a systematic study of the faceting of grain boundaries in two high density coincidence site lattices in the fcc system. Gold specimens containing grain boundaries lying in a number of predetermined orientations in the desired coincidence lattices were prepared in the form of thin-film bicrystals, and any faceting during subsequent annealing was then observed by transmission electron microscopy.

2. EXPERIMENTAL

Single crystal thin-films of gold of the required orientations were first grown on oriented single crystal rocksalt substrates using a vapor deposition method described elsewhere (Wagner 1973a). Thin-film bicrystals of the desired geometry were then obtained by pressure welding these films, while still on their substrates, together face-to-face at the required misorientation at 200°C. The misorientation between crystals and the orientation of the grain boundary plane could be controlled to within approximately ±0.5°. (for details, see Wagner 1973b.) The substrates were then dissolved away, and the thin-film bicrystals were annealed at moderate temperatures in order to equilibrate the grain boundary structure as much as possible. Extensive annealing at temperatures near the melting point could not be employed, since such treatments caused the grain boundary to migrate out of the midplane of the specimen. The resulting grain boundaries were then examined by transmission electron microscopy at normal incidence and at various oblique angles.

3. SPECIMEN GEOMETRY

Faceting was studied in two coincidences lattices, i.e., the <110>/70.5° lattice* in which Σ=3 (Fig. 1) and the

* Here we give the rotation axis and angle required to generate the coincidence lattice.

<100>/36.9^{o} lattice in which $\Sigma=5$ (Fig. 2). We note that we have constructed these coincidence lattices in Figures 1 and 2 with the lattice atoms coincident on the coincidence lattice sites (see discussion in Section 1). The boundaries which were prepared are listed in the Table and are illustrated in Figs. 1 and 2. Also listed in the Table is the corresponding planar coincidence site density parameter, Γ, which is taken as the number of coincidence sites per area a^2 of the boundary given by

$$\Gamma = \rho a^2$$

where ρ = planar density of coincidence sites, and a = lattice parameter.

4. RESULTS

The relatively low coincidence site density boundaries ACGE, AIJE and ABCD in the $\Sigma=3$ lattice were found to facet readily according to the reactions

$$\text{ACGE} \rightarrow \text{ABEF} + \text{BCGF} \quad (1)$$

$$\text{AIJE} \rightarrow \text{ABEF} + \text{BCGF} \quad (2)$$

$$\text{ABCD} \rightarrow \text{EBCH} + \text{AFGD} \quad (3)$$

The faceted structure in each case consisted of a corrugated structure (Fig. 3, top) with the facet width lying in the range 100 - 300 Å (Figs. 3 and 4). The results are summarized in the Table along with the annealing treatments which were employed.

The geometry of the faceted structure in each case was confirmed by stereomicroscopy and also by observing variations in the projected widths of the different facets as the specimen was rotated between $\pm 35^{\circ}$ around an axis parallel to the line of intersection of two adjacent facets.

In every case in reactions (1) - (3) a relatively low coincidence site density boundary decomposed into facets composed of higher coincidence site density boundaries thus confirming our expectation that the energy of a coincidence site type boundary tends to decrease with an increase in the coincidence site density, i.e., a decrease in the wave length of the periodic structure.

No faceting of the ABEF or BCGF boundaries was observed. The boundary ABEF is, of course, the classic {111} annealing twin in the fcc structure which is completely coherent and is known to have an exceedingly low energy. Numerous other electron microscopy observations have shown that this boundary remains planar as expected. The boundary BCGF is the {112} twin which also has low energy and presumably is also highly stable (see discussion to Hasson, Boos, Herbeuval, Biscondi and Goux 1972).

In the case of the $\Sigma=5$ lattice the MXYS boundary was observed to facet according to the reaction

$$\text{MXYS} \rightarrow \text{KLRP} + \text{KMSP} \qquad (4)$$

as seen in Fig. 3 (bottom). However, none of the remaining boundaries which were studied (see Table) faceted even though these boundaries were subjected to more drastic annealing treatments than were the Σ=3 boundaries (see Table). In order to reduce the probability of losing the entire boundary during the more extensive annealing treatments which were employed for these latter boundaries relatively thick bicrystal specimens were prepared (up to 1 μ thickness), and the annealed specimens were examined in the 1 MeV electron microscope at the U.S.S. Corp. Laboratory at Monroeville, Pa. We note that the faceting of the MXYS boundary was only observed in patches under conditions where large portions of the initial boundary had annealed completely out of the specimen. This result proved that the faceting reaction for this boundary was relatively sluggish and occured at a rate only slightly greater than the large scale migration of the boundary.

In many cases a third set of "cross facets" was present in the faceted structures (see Figs. 3 and 4) in order to compensate for imperfect alignment of the grain boundary plane in the coincidence lattice. A schematic drawing of a possible set of cross facets in the Σ=3 system corresponding to reaction (1) is shown in Fig. 5 for the case where the grain boundary plane has a component in the coincidence lattice plane EBCH. In this case cross facets composed of grain boundary segments running parallel to EBCH are required which produce traces which are perpendicular to the lines of intersection of the main facets.

The faceted grain boundary structure was also complicated in many cases by the presence of secondary GBD's which were present in order to compensate for deviations of the two crystals from the exact coincidence lattice misorientation. (See, for example, Fig. 4, top).

The diffraction contrast obtained from the faceted boundaries was due primarily to the formation of thickness fringes. In every observation one crystal in the bicrystal specimen was strongly excited, and thickness fringes were formed due to the periodic variation in crystal thickness due to the presence of the facets (Fig. 3, top). When both crystals were excited simultaneously with the same $\vec{g}$ vector the contrast from the facets nearly disappeared. For example, when specimens containing ACGE boundaries were tilted 35^{o} so that the common {211} was normal to the electron beam essentially no contrast from the facets was observable when either the <111> or <220> $\vec{g}$ vectors, which were common to both crystals, were employed.

4. DISCUSSION

The present results indicate that low index grain boundary planes in coincidence lattices may often decompose into a faceted structure consisting of low energy facets containing a relatively high density of coincidence sites (i.e., short wave length periodicity). The physical situation is directly analogous to the faceting of free surfaces where the surface can often reduce its energy by breaking up into a faceted structure consisting of relatively low energy facets (Herring 1951, Tracy and Blakely 1968).

The extent to which the grain boundary structures observed in the present work correspond to equilibrium structures is unknown, since only moderate annealing of the thin-film bicrystal specimens was possible without losing the boundaries by migration to the specimen surface. At any rate, the observations establish the result that the overall grain boundary energy is reduced in many cases by faceting on a fine scale (100-300Å). Faceting on this scale is, of course, far below the resolution of the light microscope and under many conditions would be difficult to detect under ordinary electron microscope observation. For example, facets of the present size would be exceedingly difficult to detect in aluminum where the extinction distances are about 4x larger than in gold. It seems likely that a coarser facet structure would have been obtained due to facet growth processes if it had been possible to anneal the specimens to higher temperatures. We also note that fine scale faceting could produce a line structure in certain grain boundaries which conceivably could be falsely attributed to GBD's.

REFERENCES

Amelinckx, S., and Dekeyser, W., 1959, Solid State Physics, 8, (Academic Press), p. 388.

Aust, K. T., 1967, Surfaces and Interfaces, I. Chemical and Physical Characteristics, edited by J. J. Burke, N. L. Reed, and V. Weiss (Syracuse University Press), p. 435.

Balluffi, R. W., Komen, Y., and Schober, T., 1972, Surf. Sci. 31, 68.

Bishop, G. H., Hartt, W. H., and Bruggeman, G. A., 1971, Acta Met., 19, 37.

Bollmann, W., 1970, Crystal Defects and Crystalline Interfaces (Springer-Verlag, New York).

Brandon, D. G., 1966, Acta Met., 14, 1479.

Bruggeman, G. A., and Bishop, G. H., 1973, J. Appl. Phys., 44, 4468.

Bruggeman, G. A., Bishop, G. H., and Hartt, W. H., 1972, The Nature and Behavior of Grain Boundaries, edited by H. Hu (Plenum Press), p. 83.

Chalmers, B., and Gleiter, H., 1971, Phil. Mag., 23, 1541.

Gleiter, H., and Chalmers, B., 1972, High-Angle Grain Boundaries (Pergamon Press), p. 13 et seq.

Hasson, G., Boos, J.-Y., Herbeuval, I., Biscondi, M., and Goux C., 1972, Surf. Sci., 31, p. 115.

Herring, C., 1951, Phys. Rev., 82, 87.

Hirth, J. P., and Balluffi, R. W., 1973, Acta Met., 21, 929.

Schober, T., and Balluffi, R. W., 1969, Phil. Mag., 20, 511; 1970, Ibid., 21, 109.

Tracy, J. C., and Blakely, J. M., 1968, Surf. Sci., 13, 313.

Wagner, W. R., 1973a, Material Science Center Report 1983, Cornell University, Ithaca, N.Y. (to be published, Surf. Sci.); 1973b, Ph.D. Thesis, Cornell University, Ithaca, N.Y.

Weinberg, F., 1969, Trans. A.I.M.E., 245, 2099.

Weins, M. J., and Weins, J. J., 1972, Phil. Mag., 26, 885.

TABLE

Faceting data for boundaries

- in the $\Sigma=3$ and $\Sigma=5$ coincidence lattices

Boundary	$\Gamma=\rho a^2$	Faceting Reaction	Annealing Treatment	Facet Width (Å)
		$\Sigma=3$		
ABEF	2.31	none	200°C,15 min	-----
BCGF	0.82	none	200°C,15 min	-----
EBCH*	0.82	----	--------	-----
ACGE	0.67	(1)	200°C,15 min	100-200
AIJE	0.47	(2)	200°C,15 min	200-300
ABCD	0.47	(3)	400°C,15 min	100-200
		$\Sigma=5$		
KLRP	0.89	none	200°C,15 min	-----
KMR*	0.68	----	-------	-----
KMSP	0.63	none	200°C,15 min	-----
KLMN	0.40	none	450°C,10 min	-----
MUVS	0.40	none	450°C,10 min	-----
MXYS	0.28	(4)	400°C,10 min	100-200

---

* Not investigated directly in present work.

FIGURE CAPTIONS

Figure 1 - Geometry of the $\Sigma=3$ system. (a) Repetitive unit of the {110} single crystals used for bicrystal fabrication. (b) Generation of bicrystal by 70.5^o, twist. (c) Unit cell of coincidence site lattice with various grain boundary planes indicated.

Figure 2 - Geometry of the $\Sigma=5$ system. (a) Repetitive unit of the {001} single crystals used for bicrystal fabrication. (b) Generation of bicrystal by 36.9^o twist. (c) Unit cell of coincidence site lattice with various grain boundaries indicated.

Figure 3 - (Top) Schematic oblique view of faceted grain boundary in bicrystal specimen. (Bottom) AIJE boundary ($\Sigma=3$) faceted according to reaction (2). Viewed along direction indicated above. Dark field: $\vec{g} = \langle 200\rangle_1$.

Figure 4 - (Top) ACGE boundary ($\Sigma=3$) faceted according to reaction (1). Dark Field: $\vec{g} = \langle 200\rangle_1$. (Middle) ABCD boundary ($\Sigma=3$) faceted according to reaction (3). Dark field: $\vec{g} = \langle 200\rangle_1$. (Bottom) MXYS boundary faceted according to reaction (4). Bright field: $\vec{g} = \langle 111\rangle_1$.

Figure 5 - Possible set of cross facets in ACGE boundary faceted according to reaction (1). (See text).

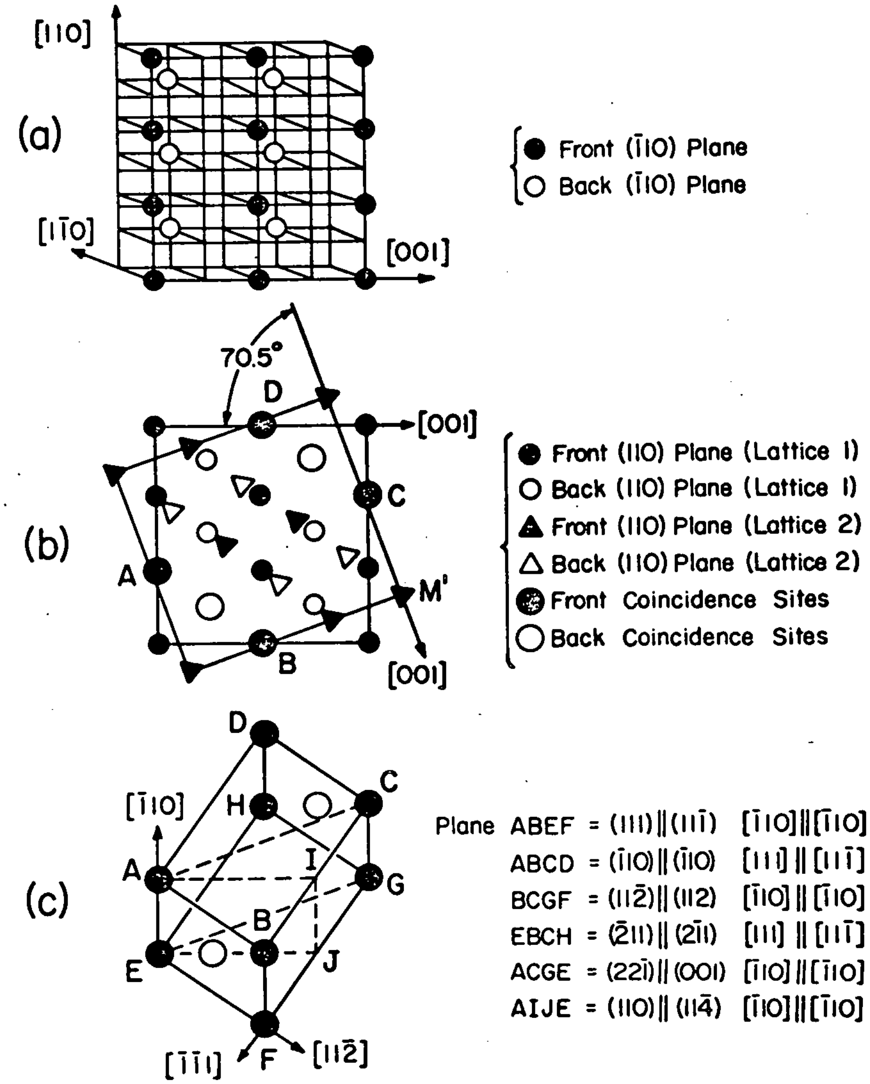

(a)
[110]
[11̄0]
[001]
Front (1̄10) Plane
Back (1̄10) Plane
(b)
70.5°
D
[001]
C
A
M'
B
[001]
Front (110) Plane (Lattice 1)
Back (110) Plane (Lattice 1)
Front (110) Plane (Lattice 2)
Back (110) Plane (Lattice 2)
Front Coincidence Sites
Back Coincidence Sites
(c)
D
C
[1̄10]
H
A
I
G
B
E
J
[1̄1̄1]
F
[112̄]
Plane ABEF = (111)||(111̄) [1̄10]||[1̄10]
ABCD = (1̄10)||(1̄10) [111]||[111̄]
BCGF = (112̄)||(112) [1̄10]||[1̄10]
EBCH = (2̄11)||(21̄1) [111]||[111̄]
ACGE = (221̄)||(001) [1̄10]||[1̄10]
AIJE = (110)||(114̄) [1̄10]||[1̄10]

Figure 1

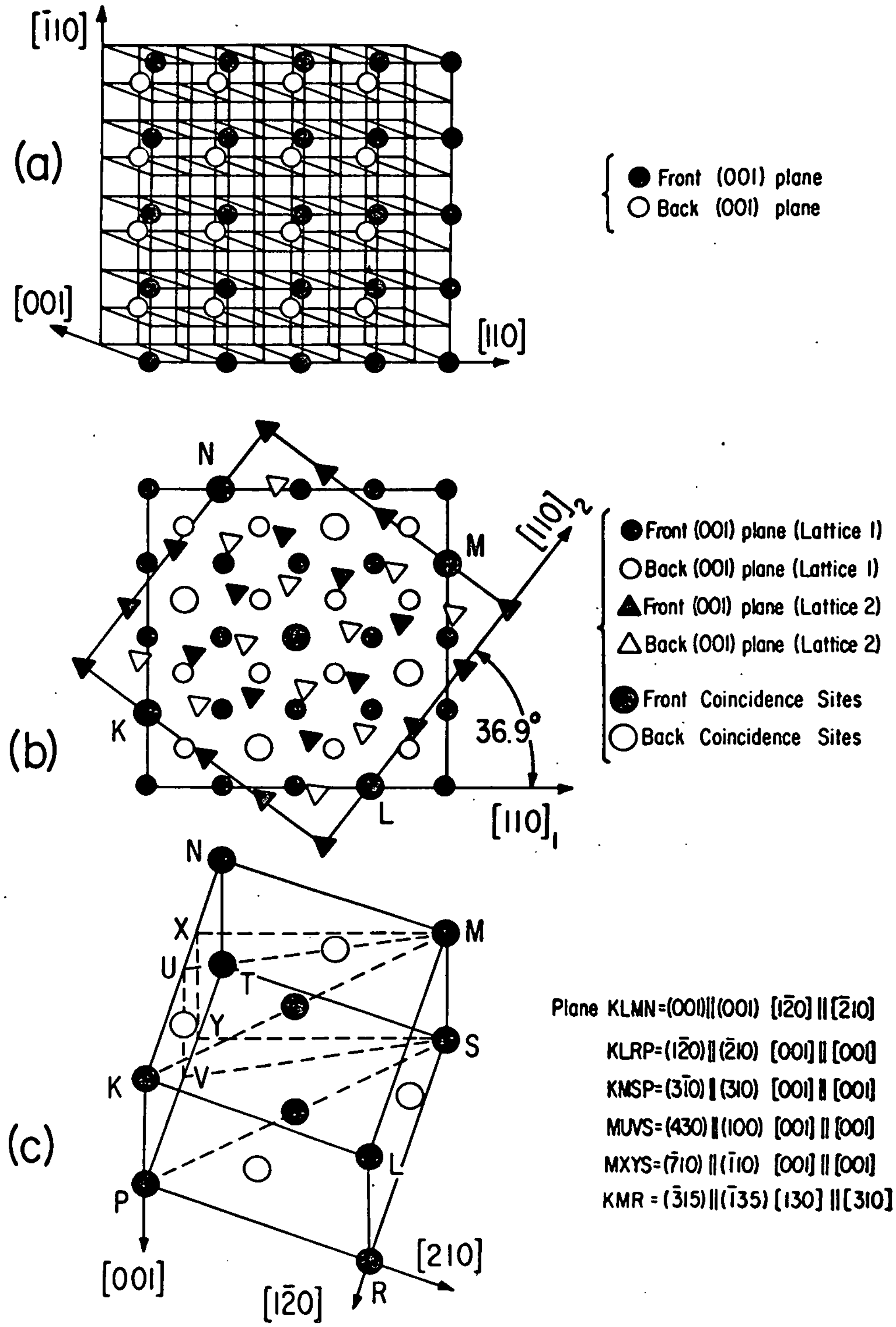

$[\bar{1}10]$
(a)
[001]
[110]
Front (001) plane
Back (001) plane
N
M
$[110]_2$
K
L
36.9°
(b)
$[110]_1$
Front (001) plane (Lattice 1)
Back (001) plane (Lattice 1)
Front (001) plane (Lattice 2)
Back (001) plane (Lattice 2)
Front Coincidence Sites
Back Coincidence Sites
N
X
M
U
T
Y
S
K
V
(c)
P
L
[001]
$[1\bar{2}0]$
R
[210]
Plane KLMN=(001)||(001) $[1\bar{2}0]$ || $[\bar{2}10]$
KLRP=$(1\bar{2}0)$||$(\bar{2}10)$ [001] || [001]
KMSP=$(3\bar{1}0)$||(310) [001] || [001]
MUVS=(430)||(100) [001] || [001]
MXYS=$(\bar{7}10)$||$(\bar{1}10)$ [001] || [001]
KMR = $(\bar{3}15)$||$(\bar{1}35)$ [130] || [310]

Figure 2

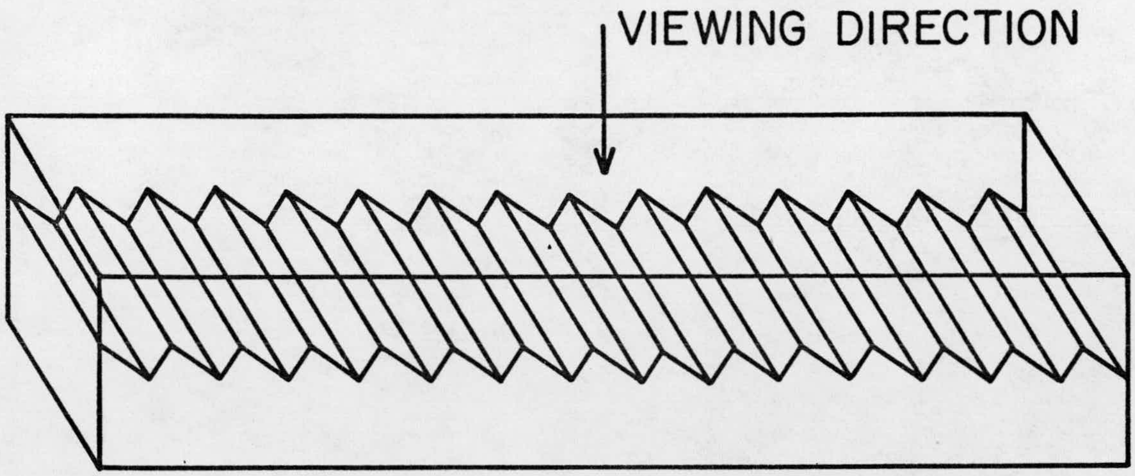

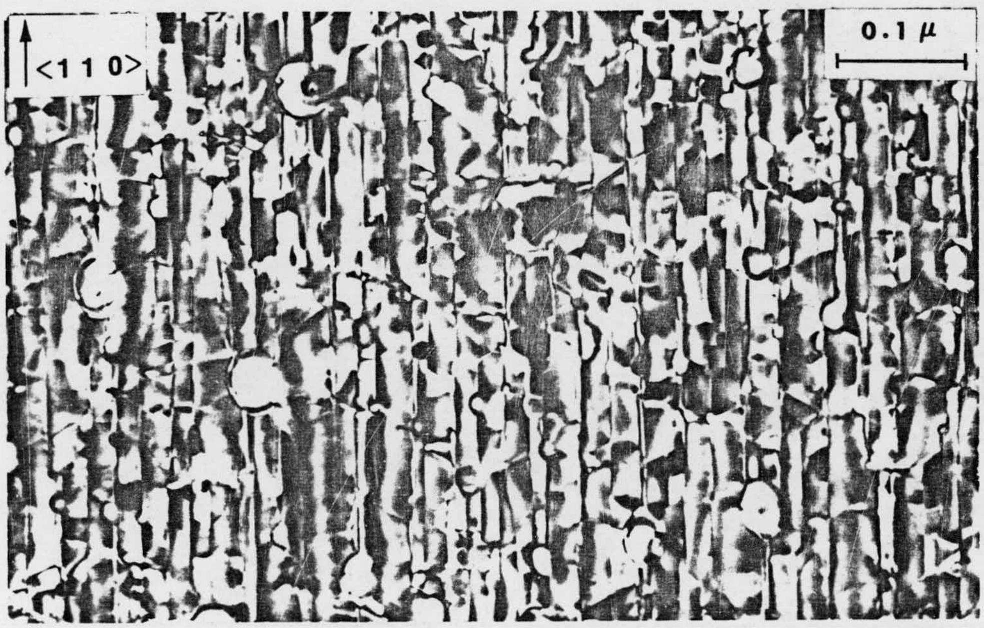

Figure 3

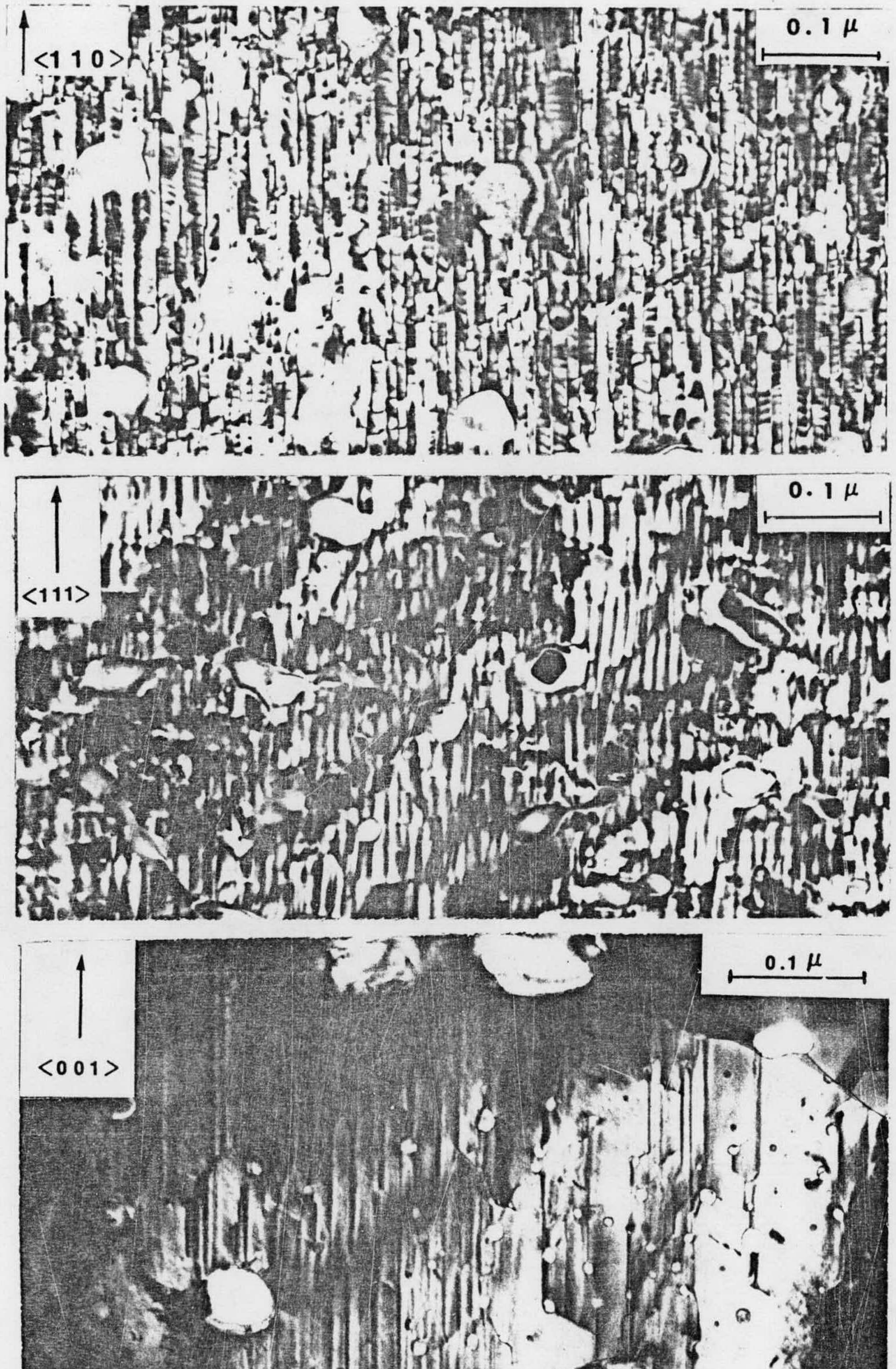

Figure 4

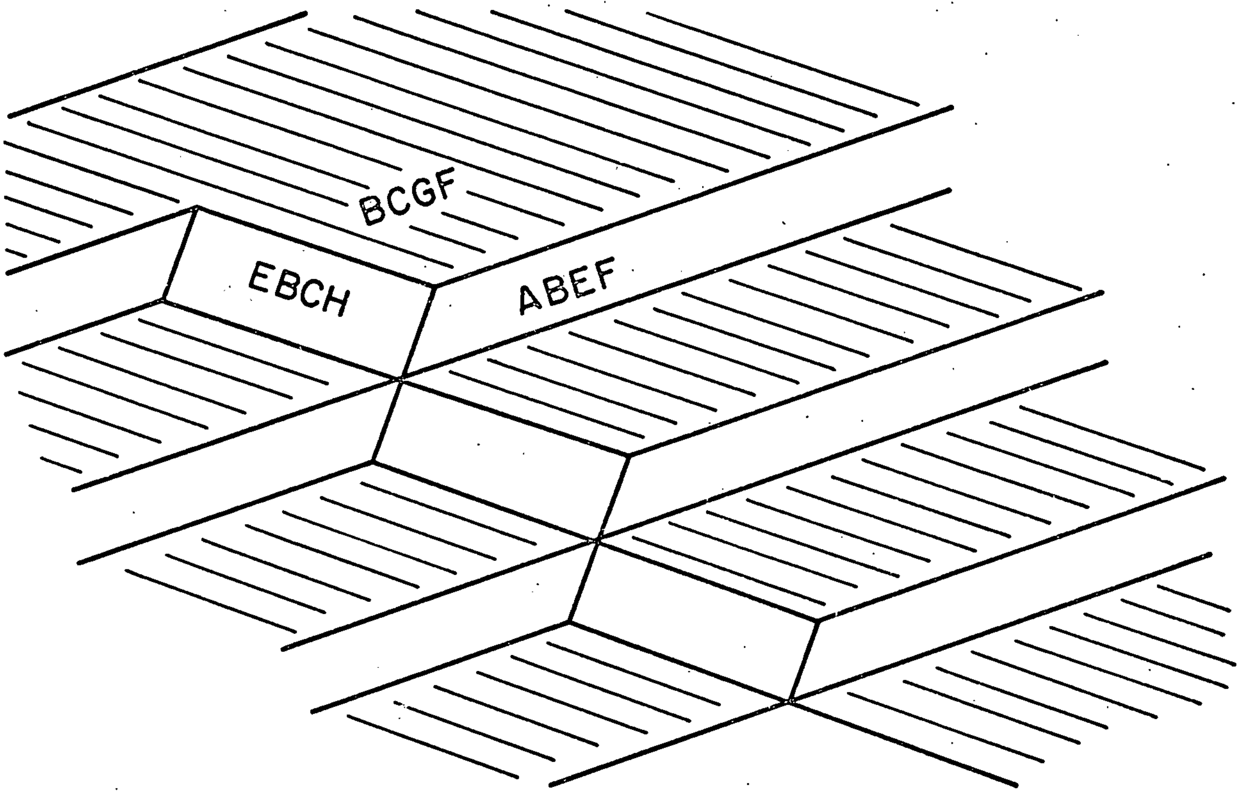

Figure 5